Chemistry & Biology
Article

Pregnenolone Functions in Centriole Cohesion during Mitosis

Mayumi Hamasaki,[1,2] Shigeru Matsumura,[1,2] Ayaka Satou,[3] Chisato Takahashi,[3] Yukako Oda,[1,2] Chika Higashiura,[1,2] Yasushi Ishihama,[3] and Fumiko Toyoshima[1,2,*]
[1]Department of Cell Biology, Institute for Virus Research, Kyoto University, Sakyo-ku, Kyoto 606-8507, Japan
[2]Department of Cell and Developmental Biology, Graduate School of Biostudies, Kyoto University, Sakyo-ku, Kyoto 606-8502, Japan
[3]Department of Molecular and Cellular BioAnalysis, Graduate School of Pharmaceutical Sciences, Kyoto University, Sakyo-ku, Kyoto 606-8501, Japan
*Correspondence: ftoyoshi@virus.kyoto-u.ac.jp
http://dx.doi.org/10.1016/j.chembiol.2014.11.005

SUMMARY

Cell division is controlled by a multitude of protein enzymes, but little is known about roles of metabolites in this mechanism. Here, we show that pregnenolone (P5), a steroid that is produced from cholesterol by the steroidogenic enzyme Cyp11a1, has an essential role in centriole cohesion during mitosis. During prometa-metaphase, P5 is accumulated around the spindle poles. Depletion of P5 induces multipolar spindles that result from premature centriole disengagement, which are rescued by ectopic introduction of P5, but not its downstream metabolites, into the cells. Premature centriole disengagement, induced by loss of P5, is not a result of precocious activation of separase, a key factor for the centriole disengagement in anaphase. Rather, P5 directly binds to the N-terminal coiled-coil domain of short-form of shugoshin 1 (sSgo1), a protector for centriole cohesion and recruits it to spindle poles in mitosis. Our results thus reveal a steroid-mediated centriole protection mechanism.

INTRODUCTION

Steroids are produced from cholesterol through a stepwise reaction of steroidogenic pathways. The first step of steroidogenic pathways is catalyzed by Cyp11a1, which cleaves the side-chain of cholesterol to produce pregnenolone (P5). P5 is then converted to 17α-hydroxypregnenolone (17-OH-P5) and progesterone (P4) by Cyp17a1 and Hsd3b, respectively, for the generation of steroid hormones (Miller, 1988). Steroids are well known to regulate homeostasis and sexual development by controlling the expression of target genes (Tomkins and Martin, 1970; Edwards, 2000). Recent reports have shown that P5 associates with microtubules and directly regulates microtubule dynamics in vitro (Murakami et al., 2000; Mizota and Ueda, 2008) and in zebrafish embryos (Hsu et al., 2006) through a nongenomic mechanism. In addition, cholesterol has been shown to actively regulate cell division (Chen et al., 1974; Fernández et al., 2004). However, the functions of steroids during cell division remain unknown.

The centrosome is the major microtubule-organization center (MTOC) in mammalian cells and organizes the poles of mitotic spindles during cell division. The centrosome consists of a pair of centrioles surrounded by pericentriolar materials (PCM) (Bornens, 2002). Centrosomes duplicate once per cell cycle, which ensures the organization of bipolar spindle poles in mitosis (Nigg, 2007; Bettencourt-Dias and Glover, 2007; Nigg and Stearns, 2011). Aberrant centrosome number, which leads to the formation of multipolar spindles, promotes genomic instability, a hallmark of cancer cells (Nigg and Raff, 2009; Fukasawa, 2007). During centrosome duplication, a new (daughter) centriole grows from the preexisting (mother) centriole during S phase. The newly formed daughter centrioles remain engaged with their mothers until late M phase. At the end of mitosis, the centrioles are disengaged, which is crucial for licensing centrioles for duplication in the next cell cycle (Kuriyama and Borisy, 1981; Tsou and Stearns, 2006; Nigg, 2007). Precise timing of centriole disengagement is crucial for accurate cell division, because precocious centriole disengagement in early mitosis causes the formation of multipolar spindles with single centrioles at each pole of the spindles, leading to defects in mitotic progression (Keryer et al., 1984; Sluder and Rieder, 1985; Hut et al., 2003).

Centriole disengagement has been shown to require the proteolytic activity of separase (Tsou and Stearns, 2006; Tsou et al., 2009), a cysteine protease known to trigger sister chromatid separation by cleaving cohesion complex subunit Scc1 (Uhlmann et al., 1999, 2000). Work from independent groups converged on a model in which separase promotes centriole disengagement in much the same way as it promotes sister chromatid separation, by cleaving Scc1, which localizes not only at centromeres but also at the spindle poles (Nakamura et al., 2009; Schöckel et al., 2011). Consistent with this model, precocious activation of separase induced by depletion of Astrin causes premature centriole disengagement (Thein et al., 2007). In addition, it has been demonstrated that separase-dependent cleavage of pericentrin, a coiled-coil protein localized in the PCM, is necessary and sufficient to induce centriole disengagement (Matsuo et al., 2012; Lee and Rhee, 2012). Although there is some debate over whether cohesin is the major substrate of separase at spindle poles during centriole disengagement (Oliveira and Nasmyth, 2013; Cabral et al., 2013), the emerging model is that separase-dependent cleavage of a centriolar "glue" protein induces centriole disengagement. In addition to separase, Polo-like kinase 1 (Plk1) has been proposed as a parallel activator for

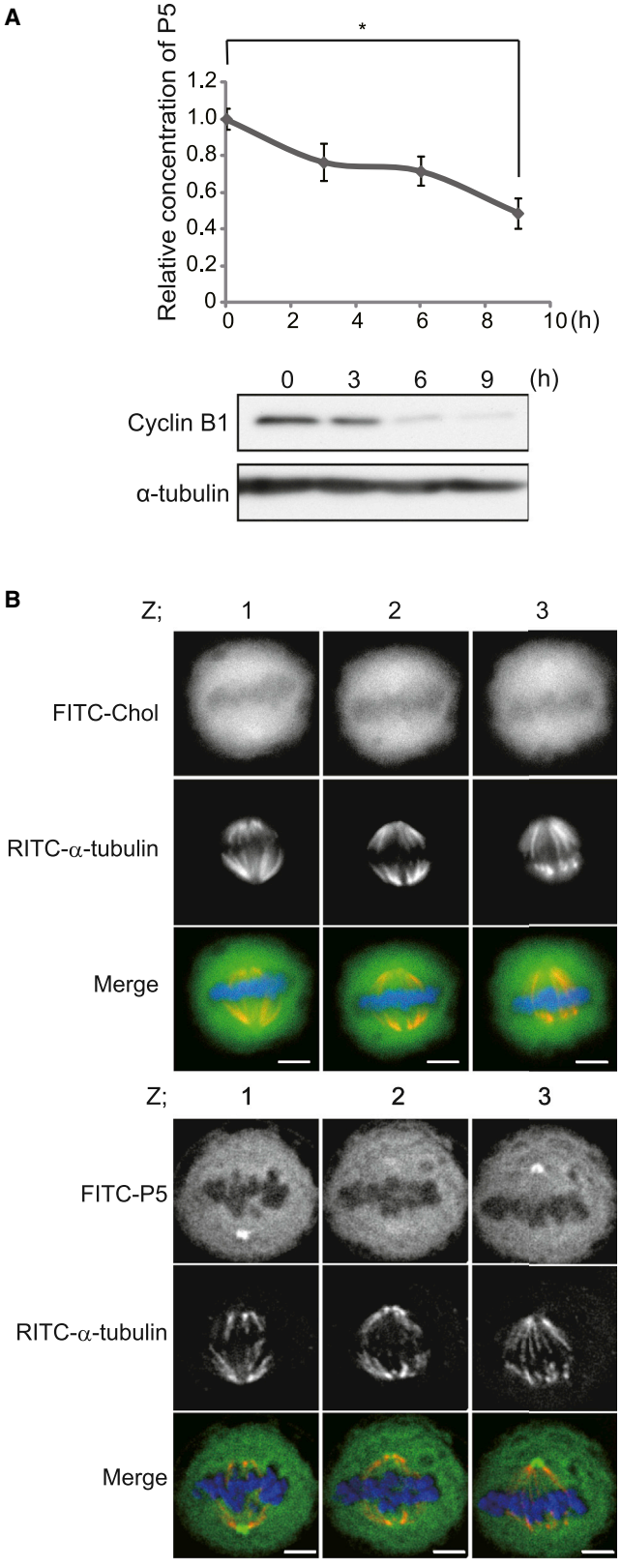

Figure 1. P5 Is Accumulated around Mitotic Spindle Poles

(A) Relative concentrations of P5 in synchronized HeLa cells after release from nocodazole arrest (upper) (mean ± SEM from six different experiments; *$p < 0.01$, analyzed by t test). Western blot of cyclin B1 and control α-tubulin (bottom).

(B) Localization of fluoresceins in prometa/metaphase cells after injection of FITC-Cholesterol (FITC-Chol) or FITC-P5 together with RITC-α-tubulin into synchronized G2 phase cells, incubated for 2 hr, and stained with Hoechst33342. Scale bars represent 1 μm. Z stack images from 0.5 μm thick sections of a metaphase cell are shown.

See also Figure S1.

centriole disengagement (Tsou et al., 2009). By analogy to sister chromatid separation, Plk1 promotes the removal of a centriolar "glue" protein, including Scc1, from the centrosomes in a separase-independent manner in early mitosis and/or facilitates anaphase-specific cleavage of the "glue" protein by separase (Tsou et al., 2009; Schöckel et al., 2011). In sister chromatid separation, the majority of cohesin is removed from chromosome arms before metaphase by the "prophase pathway," whereby Plk1 phosphorylates the SA/Scc3 cohesin subunit, triggering cohesin dissociation without its cleavage by separase (Waizenegger et al., 2000; Sumara et al., 2002). In early mitosis, centromeric cohesion is protected by shugoshin 1 (Sgo1) through direct interaction with phosphatase PP2A, which dephosphorylates SA2/Scc3 at centromeres, thereby protecting it from the prophase pathway (Kitajima et al., 2006; Riedel et al., 2006). Results from the work of Wang et al. (2008) have demonstrated that a shorter Sgo1 splice variant (sSgo1) localizes at the spindle poles and protects centriole cohesion during mitosis. What makes things complicated is that Plk1, which functions as an activator for centriole disengagement (Tsou et al., 2009; Schöckel et al., 2011), has been shown to be required for localization of sSgo1 to the spindle poles (Wang et al., 2008). Thus, the mechanisms for targeting sSgo1 at the spindle poles remain unclear.

Here, we show that P5 is accumulated around the mitotic spindle poles and functions as a protector for centriole cohesion during mitosis. Depletion of P5 induces premature centriole disengagement, which can be rescued by inhibition of Plk1 but not by inhibition of separase activation. P5 directly binds to N-terminal region of sSgo1 targets sSgo1 to the spindle poles without altering its gene expression. Furthermore, we found that Plk1 phosphorylates sSgo1 on Ser154, which ensures the spindle pole localization of sSgo1. Our results thus demonstrate an unexpected function of steroids in centriole cohesion during mitosis.

RESULTS

P5 Is Accumulated around Mitotic Spindle Poles

To gain insight into the function of P5 in cell division, we measured the cellular concentration of endogenous P5 during cell cycle. Time course experiments in HeLa cells released from nocodazole-induced M phase arrest showed the significant reduction of P5 after mitotic exit (Figure 1A). The cellular concentration of P5 was sustained through G1/S to G2/M phase (Figure S1A available online; 0–9 hr after release from a double thymidine block), but rapidly declined when the cells exited mitosis (Figure S1A; 10–12 hr). Mass spectra analysis showed that the cellular concentration of P5 in mitotic HeLa cells was 33 nM ± 4.6 (n = 3), which was much higher than that in serum (~1–3 nM) (McKenna and Brown, 1974; Ojasoo et al., 1993).

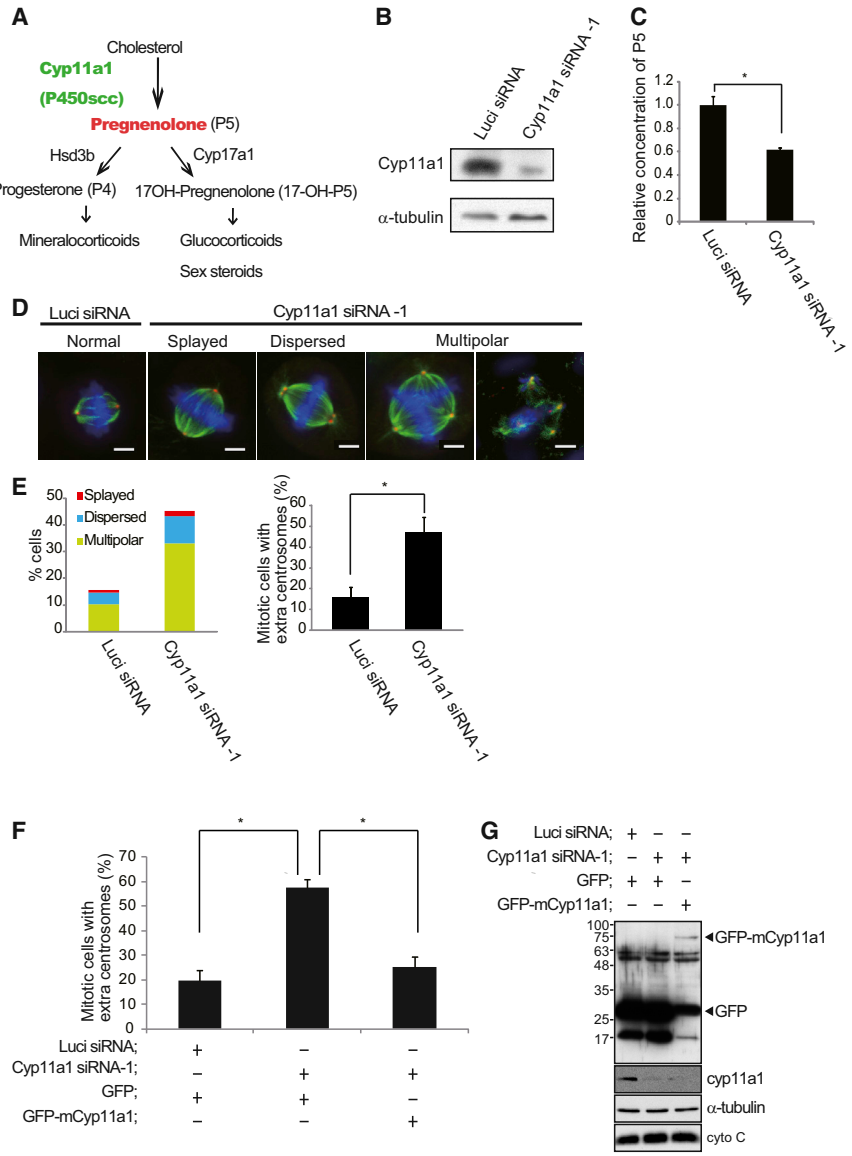

Figure 2. Knockdown of Cyp11a1 Causes Formation of Extra γ-Tubulin Foci

(A) Steroidogenic pathways.

(B) Western blot of Cyp11a1 and control α-tubulin in M phase synchronized HeLa cells transfected with Luci siRNA or Cyp11a1siRNA-1.

(C) Relative concentrations of P5 in the whole cell extracts in (B) (mean ± SEM from three different experiments; *p < 0.01, analyzed by t test).

(D) Spindle phenotypes in M phase synchronized HeLa cells, transfected with Luci siRNA or Cyp11a1 siRNA-1, stained with anti-γ-tubulin (red) and anti-α-tubulin (green) antibodies and Hoechst33342 (blue). Scale bars represent 5 μm.

(E) Percentage of mitotic cells with extra centrosomes in the cells in (D) (mean ± SEM from three different experiments; n > 100 per experiments; *p < 0.05, analyzed by t test) (right). Relative proportions of the three spindle phenotypes with extra centrosomes (left).

(F) Synchronized HeLa cells were transfected with Luci siRNA or Cyp11a1 siRNA-1 together with the plasmids encoding control GFP or GFP-mCyp11a1. Percentages of mitotic cells with extra centrosomes are shown (mean ± SEM from three different experiments; n > 50 per experiment; *p < 0.01, analyzed by Dunnett's multiple-comparison test).

(G) Western blot of GFP-mCyp11a1 (with the anti-GFP antibody), endogenous Cyp11a1, and control α-tubulin and cytochrome *c* (cyto C) in the cells in (F). Note that the anti-Cyp11a1 antibody is specific for human Cyp11a1 and does not recognize GFP-mCyp11a1.

See also Figure S2.

cluding adrenal cortex and corpus luteum (Lavoie and King, 2009), but we also detected Cyp11a1 in HeLa cells by RT-PCR and immunoblotting (Figures 2B and S2A). To investigate the functions of steroids in cell division, Cyp11a1 expression was suppressed in synchronized HeLa cells using two different small interfering RNAs (siRNAs) (Figures 2B and S2A). The cellular concentration of P5 was significantly reduced in the Cyp11a1-depleted cells, when compared to that in control cells (Figure 2C). Under this condition, mitotic cells were stained with antibodies against α-tubulin and γ-tubulin to visualize the spindles and spindle poles. In contrast to control cells in which γ-tubulin staining was intense and focused at the spindle poles, Cyp11a1-depleted cells displayed a significant increase in splayed spindle poles where γ-tubulin signals are less condensed on each spindle pole, dispersed spindle poles where two separated γ-tubulin foci are formed at each spindle pole, and multipolar spindles (Figures 2D, 2E, and S2B). The expression of mouse Cyp11a1, which is resistant to the human Cyp11a1 siRNA, restored the proper formation of spindle poles in the Cyp11a1-depleted cells, excluding possible off-target effects of the Cyp11a1 siRNAs (Figures 2F and 2G). In addition, depletion of Cyp11a1 increased a number of anaphase cells, where chromosomes were segregated toward multipolar spindle poles (Figure S2C), without

Then, the subcellular localization of P5 in mitotic cells was investigated by injecting the fluorescent dye fluorescein (FITC)-conjugated P5 (FITC-P5) (Hsu et al., 2006) (80 nM) into synchronized HeLa cells. To increase the solubility, FITC-P5 was dissolved in buffer with 3% BSA. FITC-P5 was accumulated around mitotic spindle poles, which were visualized by coinjected RITC-α-tubulin, whereas control FITC-cholesterol (FITC-Chol) was diffusely localized in the cytoplasm (Figure 1B). FITC-P5, but not FITC-Chol, displayed a spindle pole-like staining in the absence of RITC-α-tubulin (Figure S1B), excluding a possible cross talk between the channels of FITC-P5 and RITC-α-tubulin. These results prompted us to investigate the possible role of P5 in spindle organization during mitosis.

Cyp11a1 Depletion Causes Extra Centrosomal Foci in Mitotic Cells

P5 is produced from cholesterol by Cyp11a1 (Figure 2A). Cyp11a1 is highly expressed in steroid-producing cells, in-

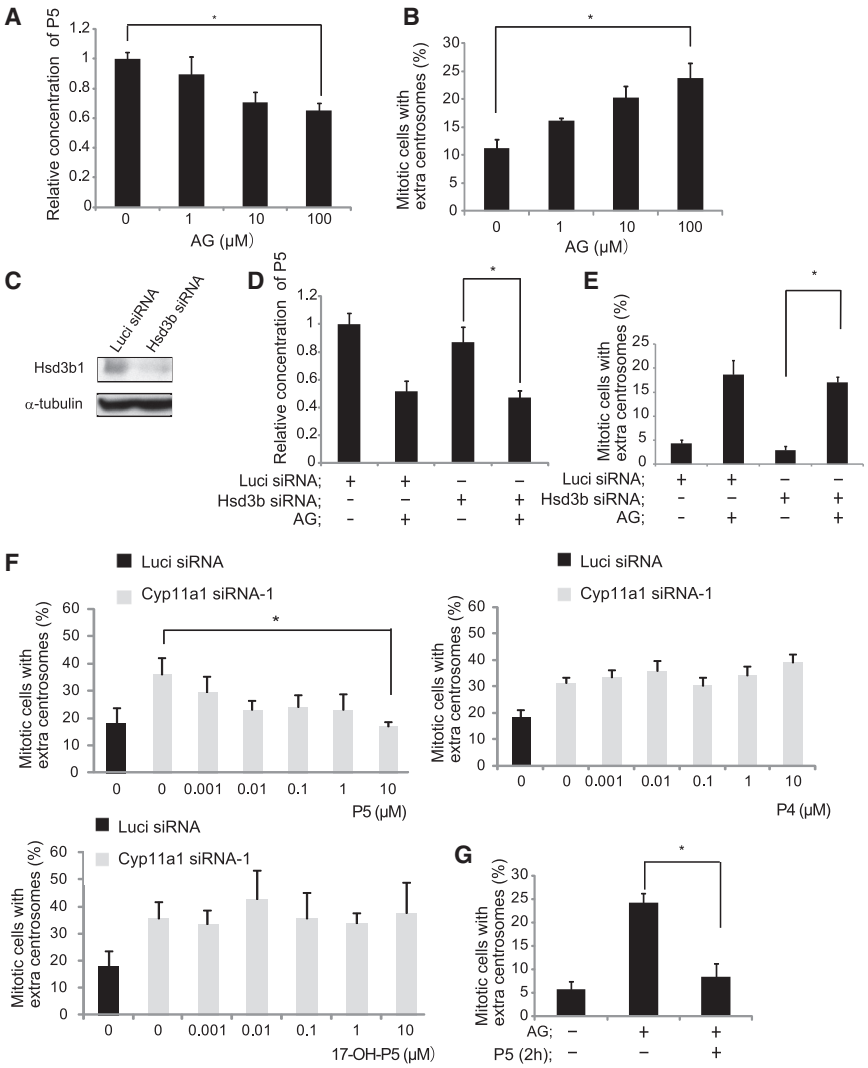

Figure 3. Cyp11a1 Depletion-Induced Formation of Extra γ-Tubulin Foci Is Suppressed by P5

(A) Relative concentrations of P5 in M phase synchronized HeLa cells incubated with or without the indicated concentrations of AG for 10 hr (mean ± SEM from three different experiments; *p < 0.01, analyzed by t test).

(B) Percentage of mitotic cells with extra centrosomes in the cells in (A) (mean ± SEM from three different experiments; n > 100 per experiments; *p < 0.05, analyzed by t test).

(C) Western blot of Hsd3b1 and control α-tubulin in M phase synchronized HeLa cells transfected with Luci siRNA or Hsd3b1 siRNA.

(D) Relative concentrations of P5 in M phase synchronized HeLa cells transfected with Luci siRNA or Hsd3b1 siRNA and incubated with or without AG (100 μM) for 10 hr (mean ± SEM from three different experiments; *p < 0.05, analyzed by t test).

(E) Percentage of mitotic cells with extra centrosomes in the cells in (D) (mean ± SEM from three different experiments; n > 100 per experiment; *p < 0.01, analyzed by t test).

(F) Percentage of mitotic cells with extra centrosomes in the cells transfected with Luci siRNA or Cyp11a1 siRNA-1 and incubated with or without the indicated concentrations of P5, P4, or 17-OH-P5 for 10 hr (mean ± SEM from three different experiments; n > 100 per experiment; *p < 0.05, analyzed by t test).

(G) Percentage of mitotic cells with extra centrosomes in the cells incubated with or without AG (100 μM) for 10 hr and further incubated with or without P5 (10 μM) for 2 hr (mean ± SEM from three different experiments; n > 100 per experiments; *p < 0.05, analyzed by t test).

See also Figure S3.

obvious increase in the number of mitotic cells (Figure S2D). Time-lapse images show that the Cyp11a1-knockdown cells, but not control cells, undergo multipolar cell division (Figures S2E and S2F). Moreover, treatment of HeLa cells with aminoglutethimide (AG), which inhibits aromatase at low doses, but at higher doses it inhibits Cyp11a1 as well (Graves and Salhanick, 1979; Uzgiris et al., 1977), for 10 hr significantly reduced the cellular concentration of P5 in a dose-dependent manner (0–100 μM) (Figure 3A) and induced extra centrosomes in mitotic cells in a correlated way (Figure 3B). From these results, we conclude that the catalytic activity of Cyp11a1 regulates spindle poles in HeLa cells.

Cyp11a1 Depletion-Induced Extra Centrosomal Foci Are Suppressed by P5

Next, we investigated whether other steroidogenic enzymes downstream of Cyp11a1 are involved in spindle pole formation. We readily detected Hsd3b protein in HeLa cells (Figure 3C), but barely detected Cyp17a1 expression (data not shown). In contrast to the Cyp11a1 depletion, knockdown of Hsd3b had only minor effect on the cellular concentration of P5 (Figure 3D) and did not induce extra centrosomal foci in mitotic cells (Figure 3E). In addition, treatment of the Hsd3b-depleted cells with AG again reduced the cellular concentration of P5 and induced extra centrosomal foci in mitotic cells (Figures 3D and 3E). Moreover, incubation of the Cyp11a1-depleted HeLa cells with P5, but not P4 or 17-OH-P5 (10 μM), for 10 hr restored the proper spindle pole formation in these cells in a dose-dependent manner (Figure 3F). Treatment of SW13 cells with these steroids (10 μM) significantly increased the cellular concentration of their downstream metabolites (estradiol for P5 and P4 and DHEA for 17-OH-P5) (Figures S3A and S3B), confirming the activity and bioavailability of these steroids. Interestingly, a short (2 hr) P5 treatment was sufficient to rescue the phenotype of extra centrosomal foci in mitosis in the AG-treated cells (Figure 3G). Thus, P5, the product of Cyp11a1, but not Cyp11a1 protein itself or downstream metabolites 17-OH-P5 or P4, regulates spindle pole formation. These results, together with the result that P5 localizes at the mitotic spindles (Figure 1B), strongly suggest that in order to avoid multipolar

cell division, P5 functions at mitotic spindles to maintain the spindle poles during mitosis.

P5 Is Required for Centriole Cohesion

The formation of additional centrosomal foci in the P5-depleted cells could result from one of two possible mechanisms: centrosome amplification or premature centriole disengagement. To examine these possibilities, cells were stained with the antibodies against centrin 2, a marker for individual centrioles, and γ-tubulin to visualize each centriole at individual spindle poles (Figure 4A). The majority of the Cyp11a1-depleted prometa/metaphase cells contained four centrioles per cell, as did control cells in the presence or absence of P5, indicating that centrosome amplification does not occur in the Cyp11a1-depleted cells (Figure 4B). Then, we quantified the number of centrioles at individual spindle poles in prometa/metaphase cells. Premature centriole disengagement will cause the formation of spindles with single centriole at individual spindle poles (Nakamura et al., 2009; Thein et al., 2007). In contrast to the spindles of control cells, which harbored two centrioles at each pole, the spindles in the Cyp11a1-depleted cells often harbored only one centriole at each pole (Figures 4A and 4C). Similar results were obtained when the cells were stained with an anticentrin antibody together with an antibody against Cep135, a maker for proximal centriole ends (Figure S4A). Moreover, incubation of the Cyp11a1-depleted cells with P5 for 10 hr restored the proper number of centrioles at each spindle pole in these cells (Figure 4C). Interestingly, Cyp11a1-depletion did not cause centriole splitting in G2 phase cells, indicating that P5 functions in the centriole cohesion mechanism in mitosis but not in G2 phase (Figure S4B). That the extra centrosomal foci induced by depletion of P5 result from premature centriole disengagement, but not from centrosome amplification, is consistent with the notion that P5 functions in maintaining centriole cohesion during mitosis.

P5 Depletion-Induced Premature Centriole Disengagement Is Suppressed by Inhibition of Plk1

Centriole disengagement requires the proteolytic activity of separase, which cleaves centriolar "glue" proteins, including cohesin and pericentrin, at late anaphase (Mardin and Schiebel, 2012). To investigate whether premature centriole disengagement is caused by the precocious activation of separase in P5-depleted cells, cells were treated with a proteasome inhibitor MG132 in order to prevent separase activation. Separase is controlled by its partner securin, which binds and inhibits separase activity (Cohen-Fix et al., 1996; Ciosk et al., 1998). At the anaphase onset, securin is ubiquitinated by the anaphase-promoting complex (APC/C), triggering securin destruction by the proteasome and thereby inducing separase activation. Thus, MG132 treatment would inhibit securin destruction, thereby preventing separase activation. In synchronized HeLa cells, separase activity, which can be monitored by the cleaved form of Kendrin (pericentrin) (Matsuo et al., 2012), was barely detected when majority of the cells were in G2/M phase (Figure 4E, 10 hr), but readily detected when the cells entered ana/telophase (Figure 4E, 13 hr). Western blot analysis for a mitotic marker Ser10-phosphorylated histone H3 confirmed that MG132 treatment effectively arrested the cells in mitosis 13 hr after release from a double thymidine block (Figure 4E). As expected, MG132 efficiently suppressed separase activation in these cells (Figure 4E). However, the spindles in the Cyp11a1-depleted prometa/metaphase cells displayed extra spindle pole foci (Figure S4C) and premature centriole disengagement (Figure 4D) even in the presence of MG132. Flow cytometric analysis of propidiumiodine-stained cells showed that the Cyp11a1-depleted cells entered into mitosis and arrested in prometaphase upon the nocodazole-treatment as in the same way as control cells (Figure S4D), excluding the possibility that the centriole disengagement in the Cyp11a1-depleted results from the tendency of these cells to slip out the metaphase arrest. In addition, Cyp11a1-depletion could induce premature centriole disengagement in the nocodazole-induced prometa/metaphase-arrested cells (Figure S4E). Furthermore, expression of YFP-Securin-ΔD, a proteasome-insensitive securin and inhibits separase activation constitutively (Hagting et al., 2002), did not suppress the premature centriole disengagement in the Cyp11a1-depleted cells (Figure 4F). These results strongly support the idea that P5 depletion-induced premature centriole disengagement does not require separase activation, although we cannot exclude the possibility that the residual (or basal) activity of separase in the MG132-treated cells or in securin-ΔD expressing cells is required for the P5 depletion-induced centriole disengagement.

Prior to separase activation, which takes place in anaphase, Plk1 activates centriole disengagement by promoting removal of a centriolar "glue" protein from centrosomes in prophase (Tsou et al., 2009; Schöckel et al., 2011). We therefore tested whether a Plk1 inhibitor BI2536 could suppress precocious centriole disengagement in Cyp11a1-depleted cells. Although BI2536 treatment slightly increased the number of mitotic cells with more than four centrioles (Figure S4F, red; compare the second column with the forth column), it efficiently suppressed the formation of extra spindle pole foci (Figure S4F, red + green) and significantly inhibited the precocious centriole disengagement in the Cyp11a1-depleted mitotic cells (Figure 4G). Western blot analysis for Ser10-phosphorylated histone H3 confirmed that both control cells and Cyp11a1-depleted cells entered into mitosis in the presence or absence of BI2536 treatment (Figure 4G). These results suggest that P5 depletion-induced premature centriole disengagement depends on the Plk1-mediated prophase pathway.

P5 Is Required for the Centrosomal Localization of sSgo1

In sister chromatid separation, centromeric cohesion at centromeres is protected from the prophase pathway by Shugoshin 1 (Sgo1), which prevents the phosphorylation and removal of cohesin at centromeres in prophase (Watanabe and Kitajima, 2005). A recent report has demonstrated that a shorter Sgo1 splice variant sSgo1 localizes to the spindle poles and functions in protecting centriole cohesion (Wang et al., 2008). We then examined the localization of sSgo1. Consistent with previous studies (Wang et al., 2006; Suzuki et al., 2006), we detected sSgo1/Sgo1 at spindle poles and kinetochores by an antibody that recognizes both sSgo1 and Sgo1 (Figure 5A). These signals were reduced to background levels in cells transfected with sSgo1/Sgo1 siRNA, which targets both sSgo1 and Sgo1, thus

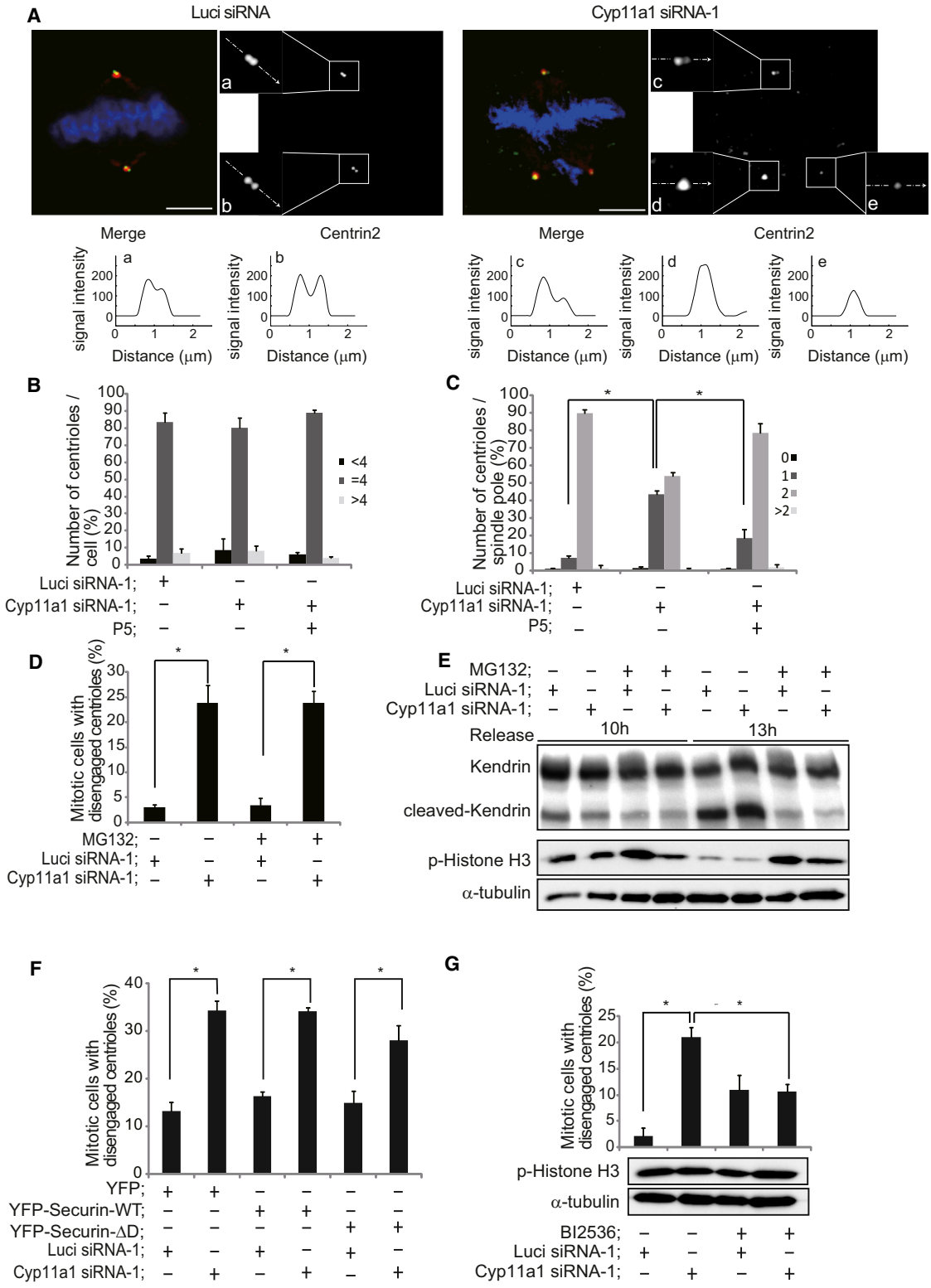

Figure 4. P5 Depletion Causes Plk1-Mediated Precocious Centriole Disengagement

(A) Images of γ-tubulin (red), centrin2 (green), and Hoechst33342 (blue) in prometa/metaphase cells transfected with Luci siRNA or Cyp11a1 siRNA-1. Images of centrin2 in boxed areas are enlarged. Scale bars represent 5 μm (upper). Signal intensities of centrin 2 on the line in a box are plotted in the bottom graph.

(B) Quantification of number of centrioles per cell in mitotic cells transfected with Luci siRNA or Cyp11a1 siRNA-1 and incubated with or without P5 (10 μM) for 10 hr (mean ± SEM from three different experiments; n > 100 per experiment).

(legend continued on next page)

validating the antibody for detection of sSgo1/Sgo1 at spindle poles and kinetochores (Figures 5A and 5B). In the Cyp11a1-depleted cells, the sSgo1/Sgo1 signals at spindle poles were significantly reduced (Figures 5C and 5D), whereas the signals at kinetochores mostly remain intact. Interestingly, incubation of the Cyp11a1-depleted cells with P5, but not P4, for 10 hr restored the spindle pole localization of sSgo1/Sgo1 in these cells (Figures 5C and 5D), indicating that P5, but not P4, is required for the spindle pole localization of Sgo1/sSgo1. Steroids are known to regulate expression of their target genes. However, the expression levels of sSgo1 protein and mRNA were not changed in the Cyp11a1-depleted cells (Figures 5B and 5E), excluding the possibility that the reduction of the sSgo1/Sgo1 signal at spindle poles results from the decrease in the expression levels.

It has been reported that the N terminus of Sgo1 localizes to spindle poles (Wang et al., 2008). Consistent with this report, GFP fused to the 158 amino acids N-terminal region of Sgo1, which is common to both Sgo1 and sSgo1 (Figure 5F, Sgo1-Nter), was correctly localized to the spindle poles (Figures 5G–5I, GFP-Sgo1-Nter). We noticed that GFP-Sgo1-Nter signals can be observed not only at spindle poles but also at kinetochores when cells were preextracted with detergent for a short period of time (20 s) before fixation (see Figure 7C). However, longer preextraction treatment (1 min) greatly decreases the signal at the kinetochore, whereas the signal at the spindle poles remain intact (Figure 5G), indicating that association of GFP-Sgo1-Nter with spindle poles is much more stable than that with kinetochores. Therefore, although signals of endogenous sSgo1/Sgo1 at kinetochores, which were resistant to the longer preextraction treatment (1 min) (Figure 5C), may represent kinetochore Sgo1, GFP-Sgo1-Nter signals at kinetochore might represent nonspecific association of this protein with nuclear/kinetochore matrix. In Cyp11a1-depleted cells, GFP-Sgo1-Nter was greatly delocalized from the spindle poles (Figures 5G–5I). Incubation of the Cyp11a1-depleted cells with P5, but not P4, again restored the localization of GFP-Sgo1-Nter at the spindle poles in these cells (Figures 5G–5I). In addition, GFP-Sgo1-Nter was readily detected in the centrosome fractions purified from control DMF-treated M phase-arrested cells, but barely detected in the centrosome fractions purified from the AG-treated M phase-arrested cells (Figure 5J). Interestingly, when the partially purified centrosome suspensions were preincubated with lipid-absorption beads before the final step of centrosome purification, GFP-Sgo1-Nter was no longer detected in the centrosome fraction, whereas it was readily detected in the centrosome fractions that were preincubated with control protein A-Sepharose beads (Figure S5A). Moreover, a short (2 hr) P5 treatment could sufficiently restore the spindle pole localization of GFP-Sgo1-Nter (Figure S5B) even in the presence of a DNA transcription suppressor actinomycin D (Figure S5C), indicating that P5-mediated spindle pole localization of GFP-Sgo1-Nter does not require de novo gene expression. From these results, we conclude that P5 promotes the localization of sSgo1 to the spindle poles through a nongenomic mechanism in order to maintain the centriole cohesion during mitosis.

P5 Binds to Sgo1-Nter

Then, what is a target protein of P5 in centriole cohesion? P5 binds to CLIP-170, a microtubule plus end-tracking protein (+Tips) to enhance its interaction with microtubules (Weng et al., 2013). Thus, it might be possible that P5 regulates centriole cohesion through CLIP-170. However, depletion of CLIP-170 by RNAi did not cause premature centriole disengagement (Figure S6B), indicating that P5 regulates centriole cohesion in a CLIP-170-independent manner. Then, we next examined whether P5 binds to sSgo1. To examine this possibility, bacterially produced MBP-Sgo1-Nter recombinant proteins or control MBP were incubated with FITC-P5 or FITC-Chol (Figure 6A and see Figure 1B). The labeled proteins were pull-down by amylose resin beads, and the FITC-fluorescence intensities in the beads were measured. The FITC signal was significantly higher in the MBP-Sgo1-Nter-conjugated beads incubated with FITC-P5 than that in the beads incubated with FITC-Chol or in the MBP-conjugated control beads (Figure 6B), indicating that P5 directly binds to Sgo1-Nter. We further truncated Sgo1-Nter (Figure 6A) and found that a small fragment at the coiled-coil region of Sgo1-Nter (residues 51–105) efficiently associates with FITC-P5 but only slightly with FITC-Chol (Figure 6B). In addition, GFP-Sgo1-Nter-(51–105), but not control GFP, was localized to the spindle poles (Figure S6A). Therefore, we identified the P5-binding region of sSgo1 in the N terminus coiled-coil domain, which is sufficient to target the protein to spindle poles.

A crystal structure of the PP2A-Sgo1 N terminus complex has shown that the coiled-coil domain within Sgo1-Nter forms a parallel homodimer, and this homodimerization is a prerequisite for PP2A binding (Xu et al., 2009). Consistent with this report, Flag-Sgo1-Nter-WT was coprecipitated with GFP-Sgo1-Nter-WT, but not with GFP-Sgo1-Nter-L68A, a mutant form of Sgo1-Nter

(C) Quantification of number of centrioles at individual spindle poles in cells treated as in (B) (mean ± SEM from three different experiments; n > 100 per experiment; *p < 0.01, analyzed by Dunnett's multiple comparison test).
(D) Percentage of mitotic cells with disengaged centrioles in the cells transfected with Luci siRNA or Cyp11a1 siRNA-1 and incubated with or without MG132 (50 μM) for 2 hr. Cells with four centrioles were analyzed (mean ± SEM from three different experiments; n > 100 per experiment; *p < 0.01, analyzed by Bonferroni procedure).
(E) Western blot analysis of Kendrin, phospho-histone H3, and control α-tubulin in synchronized HeLa cells transfected with Luci siRNA or Cyp11a1 siRNA-1 and incubated with or without MG132 (50 μM) for 2 hr (8–10 hr after release from a double thymidine block) or 5 hr (8–13 hr after the release).
(F) Percentage of mitotic cells with disengaged centrioles in M-phase synchronized cells transfected with Luci siRNA or Cyp11a1 siRNA-1 together with the plasmids encoding control YFP, YFP-Securin-WT, or YFP-Securin-ΔD (mean ± SEM from three different experiments; n > 50 per experiment; *p < 0.05, analyzed by Bonferroni procedure).
(G) Percentage of mitotic cells with disengaged centrioles in M phase synchronized cells transfected with Luci siRNA or Cyp11a1 siRNA-1 and incubated with or without BI2536 (100 nM) for 2 hr. Cells with four centrioles were analyzed (mean ± SEM from three different experiments; n > 100 per experiment; *p < 0.025, analyzed by Dunnett's multiple comparison test). Western blot analysis of phospho-histone H3 and control α-tubulin is shown at the bottom.
See also Figure S4.

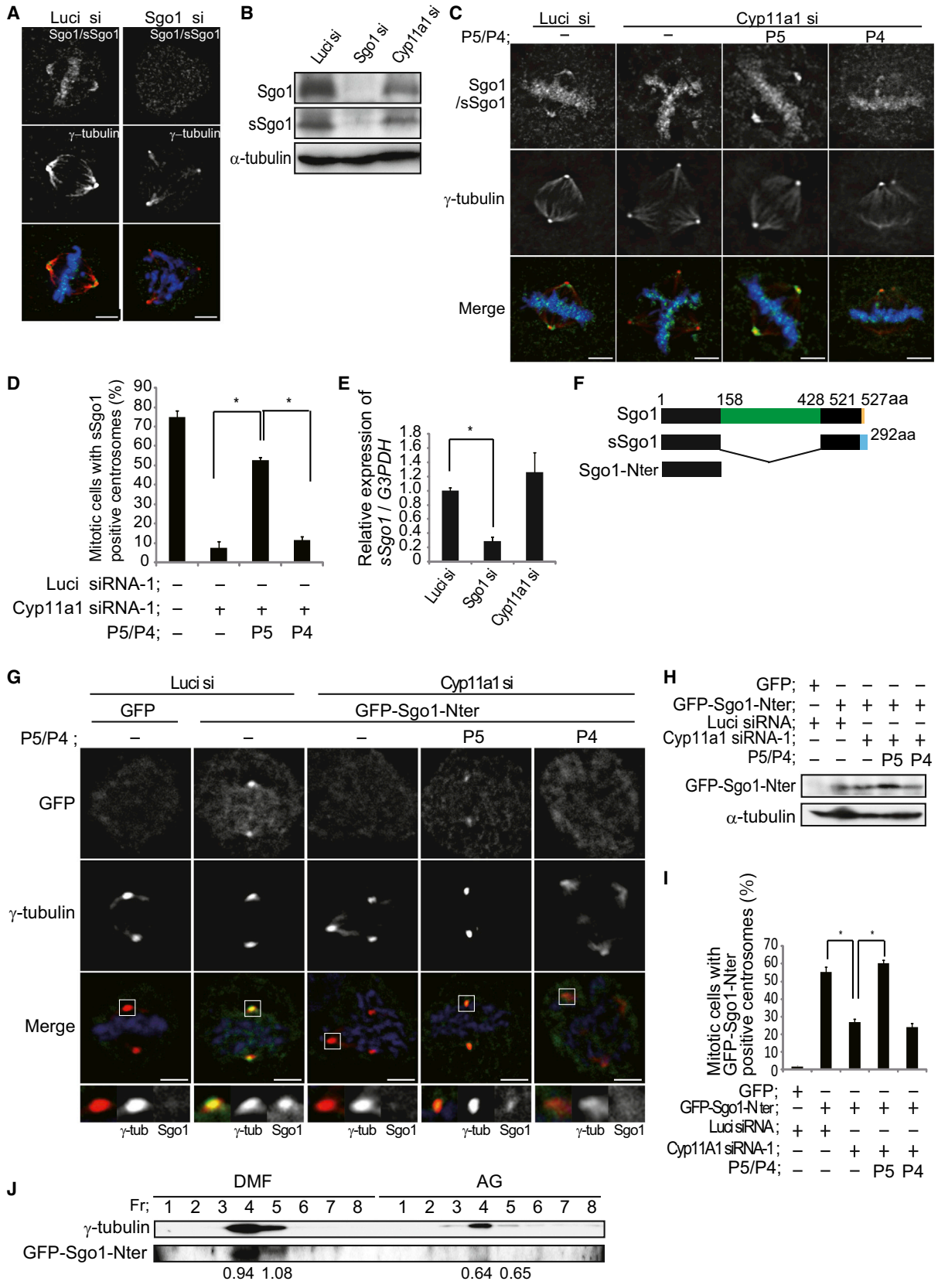

(legend on next page)

lacking homodimerization capacity (Xu et al., 2009) (Figure 6C). Interestingly, GFP-Sgo1-Nter-L68A was greatly delocalized from the spindle poles in metaphase cells (Figures 7C and 7D). This raises the possibility that P5, which promotes the spindle pole localization of sSgo1, may enhance the dimerization of Sgo1-Nter. However, it seems not to be the case, because GFP-Sgo1-Nter-WT and Flag-Sgo1-Nter-WT were coimmunoprecipitated from cells treated with or without AG in the presence or absence of P5 or P4 (Figure 6D). In addition, FITC-P5 binds to MBP-Sgo1-Nter-L68A in much the same way as MBP-Sgo1-Nter-WT (Figures 6A and 6B), indicating that homodimerization is not a prerequisite for P5 binding. Thus, both P5-binding and homodimerization of Sgo1-Nter within the coiled-coil domain ensure the spindle pole localization of sSgo1.

Plk1 Phosphorylates Sgo1-Nter on Ser154 and Enhances Its Localization at Spindle Poles

Plk1-mediated phosphorylation of sSgo1 is required for its localization to the spindle poles (Wang et al., 2008). Consistent with this report, BI2536 treatment significantly suppressed the spindle pole localization of endogenous sSgo1/Sgo1 (Figures S7C and S7D). In the Cyp11a1-depleted cells, Plk1, as well as other centrosomal proteins including Aurora A, pericentrin, and γ-tubulin, was localized to the spindle poles similar to that in control cells (Figures 7A, 7B, S7A, and S7B), excluding the possibility that Cyp11a1-depletion causes gross defects in spindle pole integrity. We then tried to identify the phosphorylation sites of sSgo1 by Plk1. Although the previous study has identified S73 and T146 as putative sites that comfort to the Plk1 phosphorylation motif (Wang et al., 2008), the evidence for the direct phosphorylation is lacking. We performed in vitro kinase assay of bacterially produced His-Plk1 using GST-Sgo1-Nter as a substrate and subjected the resultant mixture to the nano-scale liquid chromatography-tandem mass spectrometry (nanoLC-MS/MS). We did not detect the MS signal for the phosphopeptide including Ser73 nor T146 (data not shown), but did for the phosphopeptide including Ser154 (Figure 7E). In addition, in vitro kinase assay using [γ-^{32}P] ATP showed that His-WT-Plk1, but not kinase dead (KD) form of Plk1, phosphorylated GST-Sgo1-Nter, and this phosphorylation was markedly reduced when Ser154 was replaced by Ala (GST-Sgo1-Nter-S154A) (Figure 7F). In contrast, GST-Sgo1-Nter-S73A,T146A, in which both Ser73 and Thr146 were replaced by Ala, was phosphorylated by Plk1 in much the same way as GST-Sgo1-Nter-WT (Figure 7F). These results indicate that Ser154, but not Ser73 nor Thr146, is a Plk1 phosphorylation site. Importantly, Plk1 efficiently phosphorylates GST-Sgo1-Nter-L68A (Figure 7F). In addition, the phosphorylation efficiency toward GST-Sgo1-Nter did not changed even in the presence of P5 or P4 (Figure 7G). Therefore, both the homodimerization of sSgo1 and the sSgo1-P5 interaction are dispensable for the Plk1-mediated phosphorylation of sSgo1. Finally, we found that the spindle pole localization of GFP-Sgo1-Nter-S154A was significantly reduced (Figures 7C and 7D), showing that phosphorylation of Ser154 ensures the spindle pole localization of sSgo1.

DISCUSSION

This study uncovers a role of P5 in centriole cohesion in mitosis. Steroids usually act through a genomic mechanism, whereby steroids control the expression of target genes. We demonstrate that P5 regulates centriole cohesion through a nongenomic mechanism. Nongenomic function of P5 has been implicated in terminally differentiated brain tissues, whereby P5 binds to microtubule-associated protein (MAP) 2 and stimulates microtubule assembly in brain extracts and in vitro (Murakami et al., 2000; Mizota and Ueda., 2008). Recent study has shown that P5 binds to CLIP170 and promotes microtubule growth during cell migration (Weng et al., 2013). Here, we show that sSgo1 is another P5-binding protein during mitosis. Our results show that P5 directly binds to the short coiled-coil region (amino acid 51–105) of sSgo1 (Figures 6A and 6B). Although this coiled-coil region forms a homodimer that is a prerequisite for PP2A binding at kinetochore (Xu et al., 2009), the homodimerization is not necessary for its binding to P5 (Figure 6B). This outcome is not all that surprising because previous report has

Figure 5. P5 Is Required for the Spindle Pole Localization of Sgo1

(A) Images of Sgo1/sSgo1 (green), γ-tubulin (red), and Hoechst33342 (blue) in prometa/metaphase cells in M phase cells transfected with Luci siRNA or Sgo1 siRNA.

(B) Western blot analysis of Sgo1 (Sgo1), short isoform of Sgo1 (sSgo1), and control α-tubulin in the cells in (A).

(C) Images of Sgo1/sSgo1 (green), γ-tubulin (red), and Hoechst33342 (blue) in prometa/metaphase cells in M phase cells transfected with Luci siRNA or Cyp11a1 siRNA-1 and incubated with or without P5 or P4 (10 μM each) for 10 hr.

(D) Percentage of mitotic cells with Sgo1/sSgo1 positive spindle poles after treatment of the cells as in (C) (mean ± SEM from three different experiments; n > 200 per experiment; *p < 0.01, analyzed by Dunnett's multiple comparison test).

(E) qPCR analysis of sSgo1 expression in M-phase synchronized cells transfected with the indicated siRNAs. The qPCR results were normalized to the expression of *G3PDH* and compared with the control Luci siRNA-transfected cells (mean ± SEM from three different experiments; *p < 0.01, analyzed by t test).

(F) Schematic representation of the long isoform of Sgo1 (Sgo1), short isoform of Sgo1, and the N terminus region that is identical in both Sgo1 and sSgo1 (Sgo1-Nter).

(G) Localization of GFP or GFP-Sgo1-Nter in prometa/metaphase cells transfected with Luci siRNA or Cyp11a1 siRNA-1 together with plasmids encoding GFP or GFP-Sgo1-Nter and incubated with or without P5 or P4 (10 μM each) for 10 hr. Cells were preextracted with detergent for 1 min before fixation and stained with anti-GFP (green) and γ-tubulin (red) antibodies.

(H) Western blot of GFP-Sgo1-Nter and control γ-tubulin in the cells in (G).

(I) Percentage of mitotic cells with GFP-Sgo1-Nter positive spindle poles after treatment of the cells as in (G) (mean ± SEM from three different experiments; n > 200 per experiment; *p < 0.01, analyzed by Dunnett's multiple-comparison test).

(J) Centrosomes fractions purified from M phase arrested HeLa cells transfected with GFP-Sgo1-Nter, incubated with control DMF or AG (100 μM) for 18 hr. Fractions was blotted for γ-tubulin and GFP-Sgo1-Nter. The intensities of GFP-Sgo1-Nter in each fraction normalized to that of γ-tubulin are indicated at the bottom.

See also Figure S5.

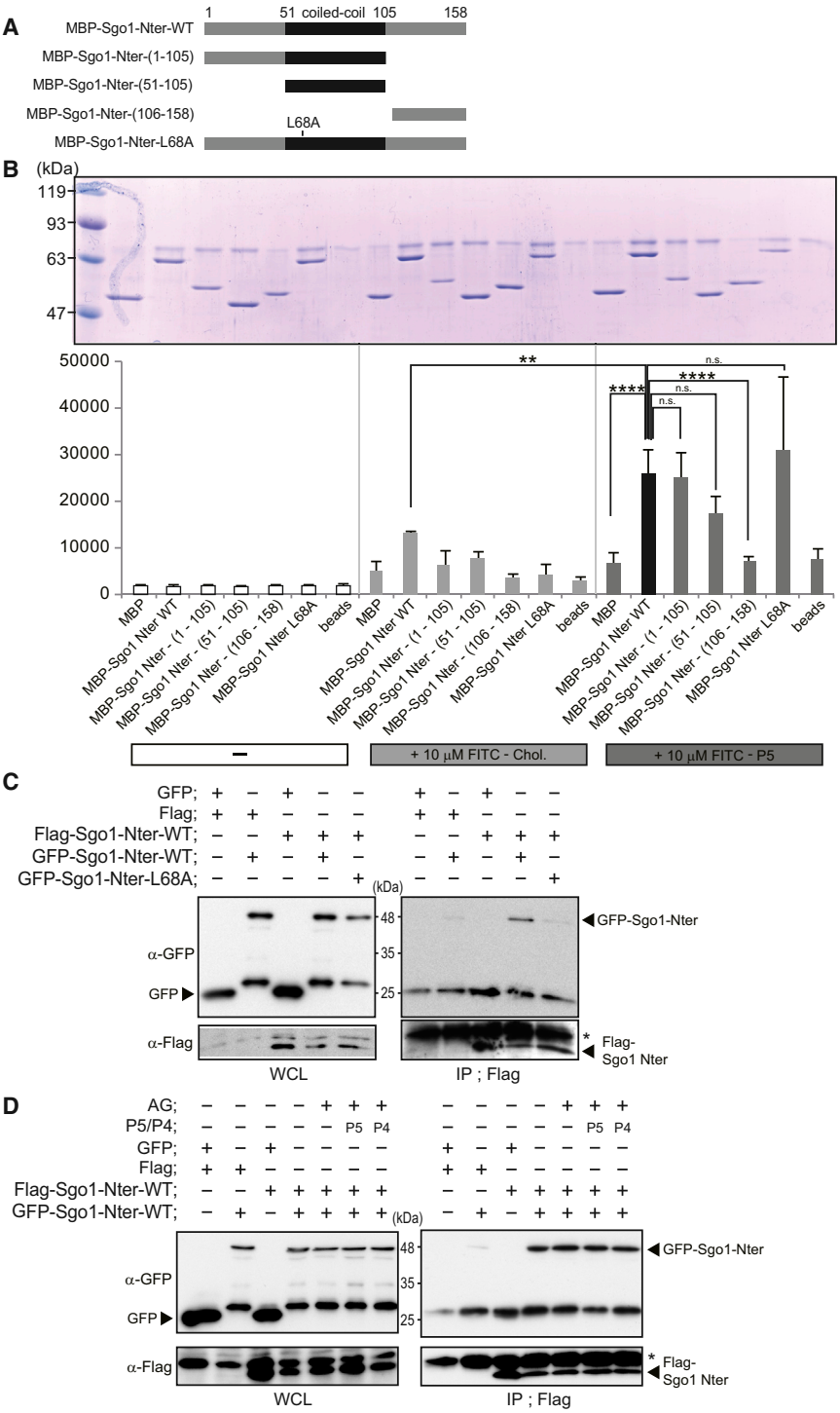

Figure 6. P5 Binds to Sgo1-Nter

(A) Doman structure of Sgo1-Nter. MBP fusions of the indicated fragments tested for the abilities to bind to FITC-P5.

(B) MBP-pull down assay of control MBP and the indicated fragments of sSgo1-Nter. Proteins (1 μg) were incubated with FITC-P5 or control FITC-Chol (100 μM) for overnight, and the resultant mixtures were incubated with amylose resin beads for 3 hr. Fluorescence intensities at 535 nm in the precipitated beads were measured by fluorescent plate reader (mean ± SEM from three different experiments; $^{**}p < 0.01$ and $^{****}p < 0.0001$, analyzed by Dunnett's multiple-comparison test). CBB staining of the precipitates are shown (upper).

(C) Coimmunoprecipitation analysis of Flag-sSgo1-Nter-WT and GFP-sSgo1-Nter-WT or GFP-sSgo1-Nter-L68A. The immunoprecipitates with anti-Flag antibody and whole cell lysates (WCL) were blotted with for anti-Flag or anti-GFP antibodies.

(D) Coimmunoprecipitation analysis of Flag-sSgo1-Nter-WT and GFP-sSgo1-Nter-WT from the M phase-synchronized HeLa cells treated with or without AG (100 μM) together with or without P5 or P4 (10 μM). The immunoprecipitates with anti-Flag antibody and whole cell lysates (WCL) were blotted with for anti-Flag or anti-GFP antibodies. See also Figure S6.

shown that bacterially produced Sgo1-Nter proteins can homodimerize in solution even in the absence P5 (Xu et al., 2009). Interestingly however, homodimerization is necessary for the spindle pole localization of sSgo1 (Figures 7C and 7D). We speculate that P5 binds to sSgo1 monomer and/or homodimer and enhance their association with a protein (protein X in Figure 7H) that recruits P5/sSgo1 complex to the vicinity of the spindle poles. At spindle poles, both homodimerization and Plk1-mediated phosphorylation on Ser154 ensure the binding of sSgo1 to a centrosomal protein(s), which might include a centriolar "glue" protein, to anchor the complexes at spindle poles (Figure 7H). Although molecular nature of the P5/sSgo1-intercating protein in the vicinity of spindle poles is unknown, binding of sSgo1 to this protein may be mitosis-specific, because P5 is required for centriole cohesion in mitotic cells, but not in G2 phase cells (Figure S4B). In addition, the cellular level of P5 is increased during mitosis (Figures 1A and S1A). The identification of this molecule as well as the structure of sSgo1-P5 complex should be clarified in future studies.

The P5 depletion-induced premature centriole disengagement is suppressed by BI2536 (Figure 4G; compare the second and forth columns), supporting the idea that the Plk1-mediated prophase pathway is required for this mechanism. However, in contrast to this finding, BI2536 treatment alone induces premature centriole disengagement (Figure 4G; compare the first and third columns) and sSgo1 delocalization from the spindle poles (Figure S7). Thus, BI2536 treatment displays dual opposing effects on the centriole disengagement: promotes centriole disengagement in control cells on one hand, and on the other hand, it suppresses centriole disengagement in the

Cyp11a1-depleted cells. This discrepancy may be due to a dual opposing role of Plk1 on centriole disengagement: Plk1 acts as a positive regulator for centriole disengagement by phosphorylating centriolar-glue proteins to remove them from centrosomes or turn them into a better substrate for separase (Tsou et al., 2009; Schöckel et al., 2011). On the other hand, Plk1 acts as a protector for centriole cohesion by phosphorylating sSgo1 to target it at the spindle poles (Wang et al., 2008). Therefore, when the control cells are treated with BI2536, sSgo1 no longer localizes to spindle poles, but the Plk1-dependent prophase pathway is also inactivated. Under this condition, the centriolar-glue proteins would be degraded by the partially activated (or the basal activity of) separase, resulting in the partial induction of premature centriole disengagement. In contrast, when the cells were depleted with Cyp11a1, sSgo1 no longer localizes to the spindle poles, whereas the Plk1-dependent prophase pathway remains active. Then, the majority of the centriolar-glue proteins would be released from the centrioles probably through Plk1-mediated phosphorylation, resulting in the significant increase in the number of mitotic cells with premature centriole disengagement, which can be suppressed efficiently by BI2536.

Does the P5-mediated centriole cohesion mechanism function ubiquitously? Cyp11a1 depletion caused the extra centrosomal foci in mitotic cells and reduced the spindle pole localization of GFP-Sgo1-Nter in adenocarcinoma A549 cells (Figures S7H–S7J). However, in nontransformed HEK293T cells, Cyp11a1 depletion did not cause the extra centrosomal foci in mitotic cells (Figures S7E and S7F). In addition, GFP-Sgo1-Nter no longer localized to spindle poles in the cells transfected with control Luci siRNA or in cells transfected with Cyp11a1 siRNAs (Figure S7G), suggesting that P5 is not necessary for centriole cohesion in HEK293. *cyp11a1* null mice died shortly after birth with symptoms of dehydration, but sustain their life to adulthood by a daily injection of corticosteroids, although they display abnormal genital tract (Hu et al., 2002). Because these mice are deficient in the synthesis of P5, P5 may be nonfunctional in centriole cohesion in nontransformed normal tissue cells. Because P5 is implicated in the cell proliferation of prostate cancer (Grigoryev et al., 2000), it might be possible that the P5-mediated centriole cohesion mechanism is one of the cell survival strategies of certain types of cancer cells. This implies that inhibition of this mechanism may induce cell death of cancer cells and thus could be a target of drug for cancer treatment.

SIGNIFICANCE

Despite the substantial progress in our knowledge on roles of proteins in cell division, little is known about a role of metabolites in this mechanism. Our results reveal a function of steroid pregnenolone in centriol cohesion during mitosis. Pregnenolone is well known as the precursor of steroid hormones, which regulate the expression of their target genes. In the centrosome regulation, however, it does not require gene expression for exerting its function. We found that pregnenolone directly binds to sSgo1 through its coiled-coil domain and targets it to centrosomes to protect centriol cohesion. Our findings would contribute to understanding how the cell metabolic state affects on the centrosome biogenesis.

EXPERIMENTAL PROCEDURES

Cell Culture and Synchronization

HeLa cells, A549 cells, and HEK293T cells were cultured in DMEM with 3%–10% fetal bovine serum. SW13 cells were cultured in DMEM/F12 with 5% fetal bovine serum. In all experiments, cells were cultured on fibronectin. Cells were synchronized in G2/M phase by the release from a double-thymidine block or were arrested in prometa/metaphase by incubating the cells with nocodazole for 18 hr.

Reagents and Antibodies

P5, P4, 17-OH-P5, and AG were purchased from Sigma. FITC-Cholesterol and RITC-tubulin were purchased from NANOCS and Cytoskeleton, respectively. FITC-P5 was chemically synthesized by Fujimoto Molecular Planning in accordance with the protocol described previously (Hsu et al., 2006). The antibodies used included anti-Cyp11a1 (ab67355, Abcam and B3997, LSBio), anti-Hsd3b (ab55658, Abcam), anti-Sgo1 (ab21633, Abcam and WH0151648M1, Sigma), anti-Plk1 (06-813, Upstate and 377000, Invitrogen), anti-Centrin2 (sc-27793-R, Santa Cruz), anti-Centrin (04-1624, Millipore), anti-Cep135 (ab75005, Abcam), anti-GFP (632381, Clontech and 04404-84, Nakalai), anti-α-tubulin (T6199, Sigma), anti-γ-tubulin (T5192 and T6557, Sigma), anti-AuroraA (610938, BD Pharmingen), anti-Pericentrin (LN#14923401, Covance), anti-Cyclin B1 (sc752, Santa Cruz), anti-cNAP1 (sc135851, Santa Cruz), and anti-Kendrin (a gift from Dr. Takahashi, Teikyo Heisei University, Ichihara, Japan).

Plasmid Constructs

mCYP11A1 was amplified with KOD-Plus-Neo (TOYOBO) using mouse ovary cDNA as a template with the following primer pairs: 5′-ATCTCGAGAT GCTGGCTAAAGGACTTTCCC-3′ and 5′-TGCTCGAGGTTCACAGTGTTGTC TTTTCTG-3′. The amplified products were subcloned into pEGFP-N1 (Clontech). pDNR-LIB-sSGO1 was purchased from Thermo Scientific. Sgo1-Nter was amplified with the primer pairs 5′-CGCGGATCCATGGCCAAGGAAA GATGCC-3′ and 5′-CGCGGATCCTTATTCTATTTGAAATGATTCTCC-3′ and subcloned into pEGFP-C1 (Clontech). YFP-securin-WT and YFP-securin-ΔD were purchased from Addgene (Hagting et al., 2002).

RNA Interference and Expression Analysis

The siRNAs targeting human Cyp11a1 were purchased from Thermo Scientific. The siRNA sequences for human Hsd3b and Sgo1 were 5′-UGU CAAUGUGAAAGGUACCUU-3′ and 5′-UGAAAGAAGCCCAAGAUAUUU-3′, respectively (Japan Bioservice). HeLa cells were transfected with siRNAs using Oligofectamine (Invitrogen), incubated for 4 hr and then synchronized by a double-thymidine block. The expression levels of Cyp11a1, Hsd3b, and Sgo1 were analyzed by western blot or RT-PCR. The expression level of *sSgo1* was analyzed by reverse transcription-quantitative polymerase chain reaction (RT-qPCR) analysis by using the following primer pairs: 5′- AGGG GACCCTTTTACAGATT-3′ and 5′- AATTGCTTCTTTGGCAGGTG-3′. The qPCR results were normalized to *G3PDH*.

Western Blot

HeLa cells were extracted with lysis buffer (20 mM HEPES, pH 7.3, 25 mM 2-glycerophosphate, 50 mM NaCl, 1.5 mM $MgCl_2$, 2mM EGTA, 0.5% Triton X-100, 2 mM DTT, 1 mM PMSF, 1 mM sodium vanadate, 2 μg/ml aprotinin, and 100 nM okadaic acid), centrifuged at 20,000 × *g* for 15 min and the supernatant was subjected to immunoblotting with anti-cyclin B1 antibodies. For western blots of Cyp11a1 and cytochrome *c*, mitochondria were purified using a mitochondria isolation kit for mammalian cells (Thermo).

Measurement of Steroids Concentration

HeLa cells and SW13 cells were extracted with lysis buffer and protein concentrations were estimated by Bradford method or by measuring the absorbance at 280 nm. The concentrations of pregnenolone, estradiol, and DHEA were measured by using a Pregnenolone-ELISA assay kit (BioVender Laboratory),

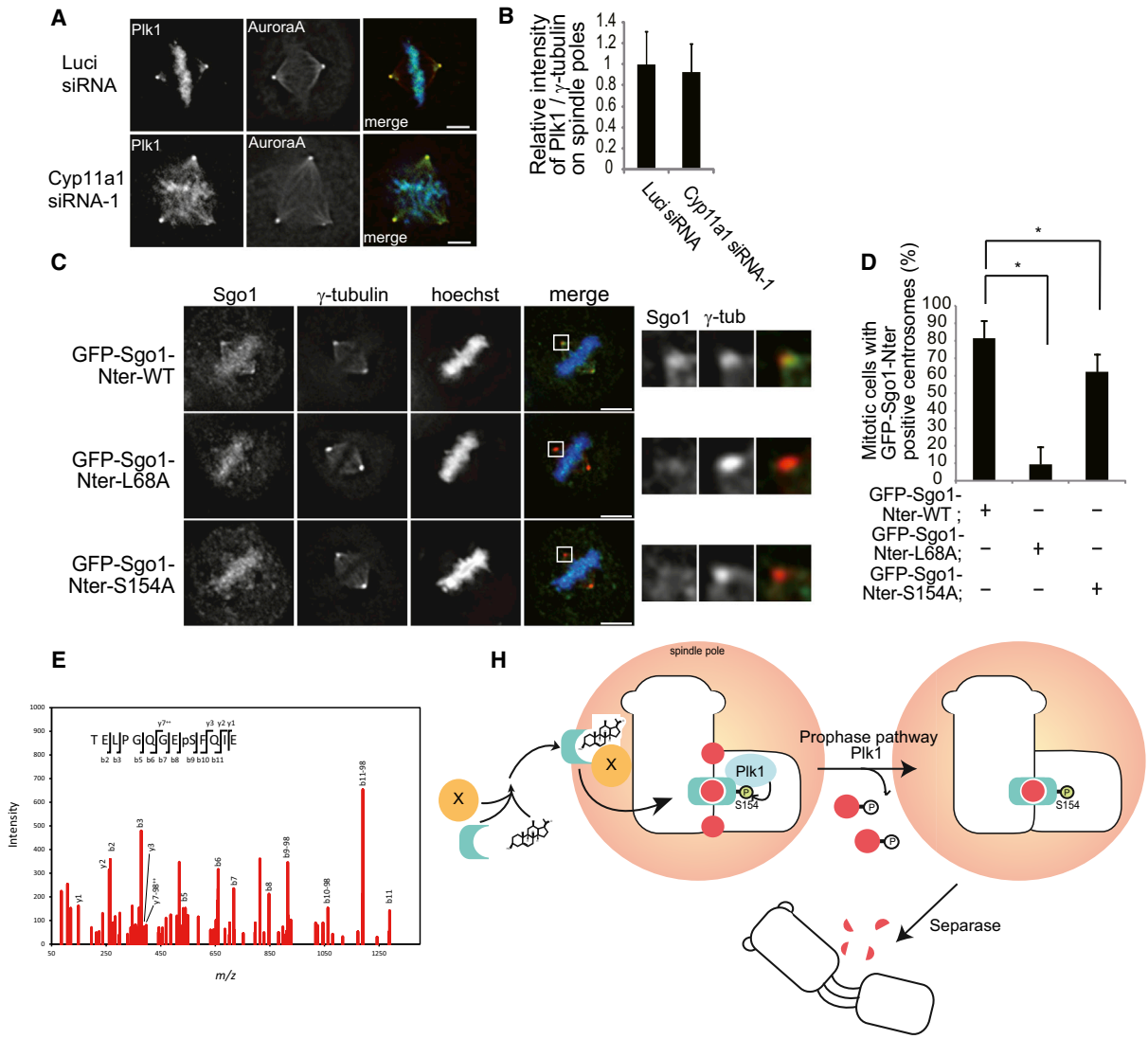

(legend on next page)

Enzyme Immunoassay kit (Cayman Chemical), and DHEA ELISA assay kit (IBL International), respectively. The results were normalized to protein concentrations.

Immunostaining

The fixation methods are as follows: α-tubulin and γ-tubulin, fixed with 3.7% formaldehyde at 37°C for 10 min, followed by incubation with methanol at −20°C for 5 min; Centrin2, Centrin, Cep135, and microinjected FITC-P5, fixed with methanol at −20°C for 2 min; AuroraA, pericentrin, endogenous sSgo1/Sgo1, GFP-Sgo1-Nter, and Plk1, preextracted in 0.5% Triton X-100 in PHEM buffer (60 mM PIPES, 25 mM HEPES, 10 mM EGTA, and 4 mM $MgSO_4$) for 20 s (Figures 5A, 5C, 7C, S7A, and S7C) or 1 min (Figure 5G), and fixed in methanol at −20°C for 5 min or 4% paraformaldehyde at 37°C 10 min. Cells were blocked with 3% BSA, incubated with primary antibodies at 4°C overnight, and incubated for 1 hr with secondary antibodies (AlexaFluor 350-, 488- or 546-goat anti-mouse, anti-rabbit, or anti-rat IgG antibodies [Molecular Probes]).

Microinjection

FITC-P5 and FITC-Cholesterol were diluted to concentrations of 10 mM in injection buffer (12 mM HEPES-KOH, pH7.5, and 120 mM KCl, 3% BSA). RITC-tubulin was dissolved in injection buffer at 4 mg/ml. The solutions were mixed together (injection buffer: FITC-P5/FITC-Cholesterol: RITC-tubulin = 3:1:1 v/v/v ratio) in a final volume of 10 μl and filtered through Millex-GV 0.22 μm filters (Millipore). The filtrates were injected in a volume of 0.1 pl in each cell into the cytoplasm of HeLa cells synchronized in G2 phase by a double-thymidine block. Microinjection was performed using an IM-188 apparatus (Narishige). After injection, cells were incubated for 2 hr to allow entry into mitosis, fixed, and stained with Hoechst33342.

Centrosome Purification

Centrosome purification was performed using a protocol modified from Moudjou and Bornens (1994). In brief, HeLa cells were transfected with GFP-Sgo1-Nter, incubated with nocodazole (250 ng/ml) for 18 hr, and further incubated with cytochalasin D (1 μg/ml) for 2 hr. Cell pellet was washed with TBS and 0.1 × TBS/8% sucrose, resuspended with 0.1 × TBS/8% sucrose and mixed with 0.5% NP-40 lysis buffer. The suspension was shaken slowly for 30 min at 4°C and spun at 2,500 × *g* for 10 min. The supernatant was added with 1 mM HEPES and 1 mg/ml DNase to make final concentrations of 10 mM and 1 μg/ml, respectively. After incubation for 30 min at 4°C, the mixture was gently underlaid with 60% sucrose solution and spun at 15,000 rpm for 30 min. The obtained centrosome suspension (partially purified centrosomes) was loaded onto a discontinuous sucrose gradient (70%, 50%, and 40% sucrose solutions from the bottom) and spun at 25,000 rpm for 1 hr. Fractions were collected by punching a small hole in the bottom of the centrifuge tube. For the lipid removal experiments, equal volumes (250 μl) of control Protein A-Sepharose beads or Cleassite (Biotech Support Group) were added to the partially purified centrosome suspensions. After incubation for 1 hr, the supernatants were subjected to the sucrose-gradient centrifugation, and centrosome fractions were obtained as described above.

Immunoprecipitation

HeLa cells were transfected with plasmids encoding Flag-Sgo1-Nter-WT and GFP-Sgo1-Nter-WT or -L68A, arrested in prometa/metaphase by 18 hr incubation with nocodazole, and treated with 1 μg/ml cytocharasin D for 1 hr. Cells were lysed in binding buffer (50 mM HEPES [pH 7.4], 10 mM 2-glycerophosphate, 50 mM NaCl, 2 mM MgCl2, 2 mM EGTA, 1 mM EDTA, 15 mM NaF, 10% glycerol, 0.5% NP-40, 5 mM dithiothreitol, 1 mM phenylmethylsulfonyl fluoride, 5 mM Na3VO4, 2 μg/ml aprotinin, and 100 nM okadaic acid), mechanically disrupted by a syringe with a 24G and 27G needle, followed by centrifugation at 12,000 rpm for 30 min. The resultant supernatants (cell extracts) were incubated with anti-Flag antibody coupled to the Protein G-Sepharose beads for 2 hr. The bead complexes were washed three times with binding buffer and subjected to immunoblotting with anti-Flag and anti-GFP antibodies.

Protein Preparation and Kinase Assay

Recombinant His-tagged mouse Plk1-WT and Plk1-KD were expressed in *Escherichia coli* and purified by affinity chromatography on Probond Resin (Invitrogen). GST-Sgo1-Nter-WT, GST-Sgo1-Nter-L68A, and GST-Sgo1-Nter-S73A/T146A were prepared by using the expression vector pGEX-6P1 (Pharmacia Biotech) and purified by affinity chromatography on glutathione-Sepharose 4B (Pharmacia). MBP-Sgo1-Nter-WT, MBP-Sgo1-Nter-(1–105), MBP-Sgo1-Nter-(51–105), MBP-Sgo1-Nter-(106–158), and MBP-Sgo1-Nter-L68A, were prepared by using the expression vector pMAL-2c (BioLabs) and purified by affinity chromatography on amylose resin (BioLabs). For phosphorylation of GST-Sgo1-Nter, purified His-tagged Plk1 proteins were mixed with GST-sSgo1-Nter proteins together with 50 μM ATP and 1.5 mM $MgCl_2$ in a final volume of 15 μl and then incubated for 20 min at 30°C in the presence of 3 μCi of [γ-^{32}P] ATP. The reactions were stopped by the adding Laemmli sample buffer and boiling.

Phosphoproteome Analysis

His-tagged and Plk1-WT and GST-Sgo1-Nter-WT were mixed together with 50 μM ATP and 1.5 mM $MgCl_2$ and incubated at 30°C for 20 min. The mixture was then digested with V8, labeled with $^{13}CH_2O$ and subjected to NanoLC-MS/MS analyses.

SUPPLEMENTAL INFORMATION

Supplemental Information includes seven figures and can be found with this article online at http://dx.doi.org/10.1016/j.chembiol.2014.11.005.

ACKNOWLEDGMENTS

We thank to Eisuke Nishida and Kunio Takeyasu (Kyoto University, Kyoto) for facilities and crucial discussions and James Hejna (Kyoto University, Kyoto) for editing and critical review of the manuscript. We thank Mikiko Takahashi (Teikyo Heisei University, Chiba) for anti-Kendrin antibodies. This work was supported by grants from the Funding Program for Next Generation World-leading Researchers (F.T., LS069), Grant-in-Aid for challenging Exploratory Research (F.T., 71714370001), Ono Medical Research Foundation (F.T.), The Sumitomo

Figure 7. Plk1 Phosphorylates Sgo-Nter on Ser154 and Localizes It at the Spindle Poles

(A) Images of Plk1 (green), AuroraA (red), and Hoechst33342 (blue) in prometa/metaphase cells transfected with Luci siRNA or Cyp11a1 siRNA-1.

(B) Relative intensities of Plk1 signals on spindle poles in prometa/metaphase cells transfected with Luci siRNA or Cyp11a1 siRNA-1. The intensities of Plk1 signals were normalized to that of γ-tubulin signals on spindle poles (mean ± SE from three different experiments; n > 20 cells per experiment).

(C) Localization of GFP-Sgo1-Nter-WT, GFP-Sgo1-Nter-L68A, or GFP-Sgo1-Nter-S154A in metaphase cells. Cells were preextracted with detergent for 1 min before fixation and stained with anti-GFP (green) and γ-tubulin (red) antibodies.

(D) Percentage of mitotic cells with GFP-positive spindle poles after transfection of the indicated plasmids as in (C) (mean ± SEM from three different experiments; n > 200 per experiment; *p < 0.01, analyzed by Dunnett's multiple-comparison test). Images of spindle poles are enlarged (right).

(E) A phosphoproteome analysis of the GST-sSgo1-Nter incubated with His tagged-Plk1-WT together with ATP and $MgCl_2$. The annotated MS/MS spectrum of TELPGQGEpSFQIE is shown.

(F) The in vitro kinase assay of His-Plk1-WT and His-Plk1-KD toward the indicated forms of GST-sSgo1-Nter. The images of CBB staining (left) and autoradiography (^{32}P; right) are shown. The normalized intensities of autoradiography are indicated at the bottom. Plk1 autophosphorylation is denoted by an asterisk.

(G) The in vitro kinase assay of His-Plk1-WT and His-Plk1-KD toward GST-sSgo1-Nter in the presence or absence of the indicated concentrations of P5 or P4.

(H) A model for the P5-mediated centriole engagement.

See also Figure S7.

Foundation (F.T.), The Mitsubishi Foundation (F.T.), and Astellas Foundation for Research on Metabolic Disorders (F.T.).

Received: August 7, 2014
Revised: October 26, 2014
Accepted: November 3, 2014
Published: December 18, 2014

REFERENCES

Bettencourt-Dias, M., and Glover, D.M. (2007). Centrosome biogenesis and function: centrosomics brings new understanding. Nat. Rev. Mol. Cell Biol. *8*, 451–463.

Bornens, M. (2002). Centrosome composition and microtubule anchoring mechanisms. Curr. Opin. Cell Biol. *14*, 25–34.

Cabral, G., Sans, S.S., Cowan, C.R., and Dammermann, A. (2013). Multiple mechanisms contribute to centriole separation in C. elegans. Curr. Biol. *23*, 1380–1387.

Chen, H.W., Kandutsch, A.A., and Waymouth, C. (1974). Inhibition of cell growth by oxygenated derivatives of cholesterol. Nature *251*, 419–421.

Ciosk, R., Zachariae, W., Michaelis, C., Shevchenko, A., Mann, M., and Nasmyth, K. (1998). An ESP1/PDS1 complex regulates loss of sister chromatid cohesion at the metaphase to anaphase transition in yeast. Cell *93*, 1067–1076.

Cohen-Fix, O., Peters, J.M., Kirschner, M.W., and Koshland, D. (1996). Anaphase initiation in Saccharomyces cerevisiae is controlled by the APC-dependent degradation of the anaphase inhibitor Pds1p. Genes Dev. *10*, 3081–3093.

Edwards, D.P. (2000). The role of coactivators and corepressors in the biology and mechanism of action of steroid hormone receptors. J. Mammary Gland Biol. Neoplasia *5*, 307–324.

Fernández, C., Lobo Md, Mdel.V., Gómez-Coronado, D., and Lasunción, M.A. (2004). Cholesterol is essential for mitosis progression and its deficiency induces polyploid cell formation. Exp. Cell Res. *300*, 109–120.

Fukasawa, K. (2007). Oncogenes and tumour suppressors take on centrosomes. Nat. Rev. Cancer *7*, 911–924.

Graves, P.E., and Salhanick, H.A. (1979). Stereoselective inhibition of aromatase by enantiomers of aminoglutethimide. Endocrinology *105*, 52–57.

Grigoryev, D.N., Long, B.J., Njar, V.C., and Brodie, A.H. (2000). Pregnenolone stimulates LNCaP prostate cancer cell growth via the mutated androgen receptor. J. Steroid Biochem. Mol. Biol. *75*, 1–10.

Hagting, A., Den Elzen, N., Vodermaier, H.C., Waizenegger, I.C., Peters, J.M., and Pines, J. (2002). Human securin proteolysis is controlled by the spindle checkpoint and reveals when the APC/C switches from activation by Cdc20 to Cdh1. J. Cell Biol. *157*, 1125–1137.

Hsu, H.J., Liang, M.R., Chen, C.T., and Chung, B.C. (2006). Pregnenolone stabilizes microtubules and promotes zebrafish embryonic cell movement. Nature *439*, 480–483.

Hu, M.C., Hsu, N.C., El Hadj, N.B., Pai, C.I., Chu, H.P., Wang, C.K., and Chung, B.C. (2002). Steroid deficiency syndromes in mice with targeted disruption of Cyp11a1. Mol. Endocrinol. *16*, 1943–1950.

Hut, H.M., Lemstra, W., Blaauw, E.H., Van Cappellen, G.W., Kampinga, H.H., and Sibon, O.C. (2003). Centrosomes split in the presence of impaired DNA integrity during mitosis. Mol. Biol. Cell *14*, 1993–2004.

Keryer, G., Ris, H., and Borisy, G.G. (1984). Centriole distribution during tripolar mitosis in Chinese hamster ovary cells. J. Cell Biol. *98*, 2222–2229.

Kitajima, T.S., Sakuno, T., Ishiguro, K., Iemura, S., Natsume, T., Kawashima, S.A., and Watanabe, Y. (2006). Shugoshin collaborates with protein phosphatase 2A to protect cohesin. Nature *441*, 46–52.

Kuriyama, R., and Borisy, G.G. (1981). Centriole cycle in Chinese hamster ovary cells as determined by whole-mount electron microscopy. J. Cell Biol. *91*, 814–821.

Lavoie, H.A., and King, S.R. (2009). Transcriptional regulation of steroidogenic genes: STARD1, CYP11A1 and HSD3B. Exp. Biol. Med. (Maywood) *234*, 880–907.

Lee, K., and Rhee, K. (2012). Separase-dependent cleavage of pericentrin B is necessary and sufficient for centriole disengagement during mitosis. Cell Cycle *11*, 2476–2485.

Mardin, B.R., and Schiebel, E. (2012). Breaking the ties that bind: new advances in centrosome biology. J. Cell Biol. *197*, 11–18.

Matsuo, K., Ohsumi, K., Iwabuchi, M., Kawamata, T., Ono, Y., and Takahashi, M. (2012). Kendrin is a novel substrate for separase involved in the licensing of centriole duplication. Curr. Biol. *22*, 915–921.

McKenna, T.J., and Brown, R.D. (1974). Pregnenolone in man: plasma levels in states of normal and abnormal steroidogenesis. J. Clin. Endocrinol. Metab. *38*, 480–485.

Miller, W.L. (1988). Molecular biology of steroid hormone synthesis. Endocr. Rev. *9*, 295–318.

Mizota, K., and Ueda, H. (2008). N-terminus of MAP2C as a neurosteroid-binding site. Neuroreport *19*, 1529–1533.

Moudjou, M., and Bornens, M. (1994). Isolation of centrosomes from cultured animal cells. In Cell Biology: A Laboratory Handbook, J.E. Celis, ed. (Waltham, MA: Academic Press), pp. 595–604.

Murakami, K., Fellous, A., Baulieu, E.E., and Robel, P. (2000). Pregnenolone binds to microtubule-associated protein 2 and stimulates microtubule assembly. Proc. Natl. Acad. Sci. USA *97*, 3579–3584.

Nakamura, A., Arai, H., and Fujita, N. (2009). Centrosomal Aki1 and cohesin function in separase-regulated centriole disengagement. J. Cell Biol. *187*, 607–614.

Nigg, E.A. (2007). Centrosome duplication: of rules and licenses. Trends Cell Biol. *17*, 215–221.

Nigg, E.A., and Raff, J.W. (2009). Centrioles, centrosomes, and cilia in health and disease. Cell *139*, 663–678.

Nigg, E.A., and Stearns, T. (2011). The centrosome cycle: Centriole biogenesis, duplication and inherent asymmetries. Nat. Cell Biol. *13*, 1154–1160.

Ojasoo, T., Fiet, J., Raynaud, J.P., and Doré, J.C. (1993). A multivariate approach to the description of patient populations. An example of the analysis of the hormone profiles of patients with advanced prostate cancer. J. Steroid Biochem. Mol. Biol. *46*, 183–193.

Oliveira, R.A., and Nasmyth, K. (2013). Cohesin cleavage is insufficient for centriole disengagement in Drosophila. Curr. Biol. *23*, R601–R603.

Riedel, C.G., Katis, V.L., Katou, Y., Mori, S., Itoh, T., Helmhart, W., Gálová, M., Petronczki, M., Gregan, J., Cetin, B., et al. (2006). Protein phosphatase 2A protects centromeric sister chromatid cohesion during meiosis I. Nature *441*, 53–61.

Schöckel, L., Möckel, M., Mayer, B., Boos, D., and Stemmann, O. (2011). Cleavage of cohesin rings coordinates the separation of centrioles and chromatids. Nat. Cell Biol. *13*, 966–972.

Sluder, G., and Rieder, C.L. (1985). Centriole number and the reproductive capacity of spindle poles. J. Cell Biol. *100*, 887–896.

Sumara, I., Vorlaufer, E., Stukenberg, P.T., Kelm, O., Redemann, N., Nigg, E.A., and Peters, J.M. (2002). The dissociation of cohesin from chromosomes in prophase is regulated by Polo-like kinase. Mol. Cell *9*, 515–525.

Suzuki, H., Akiyama, N., Tsuji, M., Ohashi, T., Saito, S., and Eto, Y. (2006). Human Shugoshin mediates kinetochore-driven formation of kinetochore microtubules. Cell Cycle *5*, 1094–1101.

Thein, K.H., Kleylein-Sohn, J., Nigg, E.A., and Gruneberg, U. (2007). Astrin is required for the maintenance of sister chromatid cohesion and centrosome integrity. J. Cell Biol. *178*, 345–354.

Tomkins, G.M., and Martin, D.W., Jr. (1970). Hormones and gene expression. Annu. Rev. Genet. *4*, 91–106.

Tsou, M.F., and Stearns, T. (2006). Mechanism limiting centrosome duplication to once per cell cycle. Nature *442*, 947–951.

Tsou, M.F., Wang, W.J., George, K.A., Uryu, K., Stearns, T., and Jallepalli, P.V. (2009). Polo kinase and separase regulate the mitotic licensing of centriole duplication in human cells. Dev. Cell *17*, 344–354.

Uhlmann, F., Lottspeich, F., and Nasmyth, K. (1999). Sister-chromatid separation at anaphase onset is promoted by cleavage of the cohesin subunit Scc1. Nature *400*, 37–42.

Uhlmann, F., Wernic, D., Poupart, M.A., Koonin, E.V., and Nasmyth, K. (2000). Cleavage of cohesin by the CD clan protease separin triggers anaphase in yeast. Cell *103*, 375–386.

Uzgiris, V.I., Whipple, C.A., and Salhanick, H.A. (1977). Stereoselective inhibition of cholesterol side chain cleavage by enantiomers of aminoglutethimide. Endocrinology *101*, 89–92.

Waizenegger, I.C., Hauf, S., Meinke, A., and Peters, J.M. (2000). Two distinct pathways remove mammalian cohesin from chromosome arms in prophase and from centromeres in anaphase. Cell *103*, 399–410.

Wang, X., Yang, Y., and Dai, W. (2006). Differential subcellular localizations of two human Sgo1 isoforms: implications in regulation of sister chromatid cohesion and microtubule dynamics. Cell Cycle *5*, 635–640.

Wang, X., Yang, Y., Duan, Q., Jiang, N., Huang, Y., Darzynkiewicz, Z., and Dai, W. (2008). sSgo1, a major splice variant of Sgo1, functions in centriole cohesion where it is regulated by Plk1. Dev. Cell *14*, 331–341.

Watanabe, Y., and Kitajima, T.S. (2005). Shugoshin protects cohesin complexes at centromeres. Philos. Trans. R. Soc. Lond. B Biol. Sci. *360*, 515–521, discussion 521.

Weng, J.H., Liang, M.R., Chen, C.H., Tong, S.K., Huang, T.C., Lee, S.P., Chen, Y.R., Chen, C.T., and Chung, B.C. (2013). Pregnenolone activates CLIP-170 to promote microtubule growth and cell migration. Nat. Chem. Biol. *9*, 636–642.

Xu, Z., Cetin, B., Anger, M., Cho, U.S., Helmhart, W., Nasmyth, K., and Xu, W. (2009). Structure and function of the PP2A-shugoshin interaction. Mol. Cell *35*, 426–441.